Morphotropic $NaNbO_3$-$BaTiO_3$-$CaZrO_3$ lead-free ceramics with temperature-insensitive piezoelectric properties

Ruzhong Zuo,[a] He Qi, and Jian Fu
Institute of Electro Ceramics and Devices, School of Materials Science and Engineering, Hefei University of Technology, Hefei, 230009, People's Republic of China

(Received 26 May 2016; accepted 5 July 2016; published online 15 July 2016)

A morphotropic $NaNbO_3$-based lead-free ceramic was reported to have temperature-insensitive piezoelectric and electromechanical properties ($d_{33} = 231$ pC/N, $k_p = 35\%$, $T_c = 148\,^\circ$C, and low-hysteresis strain ~0.15%) in a relatively wide temperature range. This was fundamentally ascribed to the finding of a composition-axis vertical morphotropic phase boundary in which coexisting ferroelectric phases are only compositionally driven and thermally insensitive. Both phase coexistence and nano-scaled domain morphology deserved well enhanced electrical properties, as evidenced by means of synchrotron x-ray diffraction and transmission electron microscopy. Our study suggests that the current lead-free ceramic would be a very promising piezoelectric material for actuator and sensor applications. *Published by AIP Publishing*. [http://dx.doi.org/10.1063/1.4958937]

Lead-free piezoelectric materials are mainly based on perovskite-structured solid solutions chemically designed close to the boundary of two ferroelectric phases of different symmetries,[1,2] which straightforwardly decides ultimate electromechanical properties and especially their thermal stability. Traditional Pb(Zr,Ti)O_3 (PZT) based materials have been applied basically as a result of a compositionally driven ferroelectric rhombohedral (R)-tetragonal (T) morphotropic phase boundary (MPB), which is nearly vertical to the composition coordinate axis.[3] This provides a solid structural fundament for achieving stable electromechanical properties of devices in service in a wide temperature range. Typical lead-free piezoelectric systems based on $(Bi_{0.5}Na_{0.5})TiO_3$ (BNT), $BaTiO_3$ (BT), or $(Na_{0.5}K_{0.5})NbO_3$ (NKN) so far reported achieved significantly enhanced piezoelectric properties through lots of efforts, some of which have been comparable to those of PZT systems.[4–7] However, the thermal stability of piezoelectric properties has been seriously challenged by at least one of the following two aspects. One is a relatively low Curie point (T_c) or low depolarization temperature (T_d) such as BNT-based systems ($T_d < 100\,^\circ$C) and modified BT systems ($T_d < 80\,^\circ$C).[8,9] The other one is the polymorphic phase boundary (PPB) at which the transformation between coexisting phases (R, T, or orthorhombic (O)) can be driven by not only composition but also temperature in the case of BT-based and NKN-based compounds.[6,10–14] As a consequence, the PPB is mostly rather tilted relative to the composition axis in a composition-temperature phase diagram, which intrinsically induced a significant temperature dependence of electrical properties.[9,15,16] Although a vertical phase boundary was claimed,[17,18] there still lacked clear evidences of the morphotropism nature as well as temperature-insensitive piezoelectric properties.

In perovskite-structured material systems of forming solid solutions, the increased inner energies because of the mismatch of lattices need to be released as one crystal structure dissolved into another one. Therefore, these two kinds of lattices probably take the way to reach a relatively stable energy state by separately existing (coexisting) at a more microscopic scale (for example, nanostructures)[19–21] in some cases, instead of still forming a single phase merely by changing the lattice distortion degree, thereby producing a composition driven phase boundary (i.e., MPB). However, the situation may be changed where the material system with multiple thermally excited phase structure transitions (i.e., polymorphic phase transition, PPT) below T_c can reduce inner energies under these circumstances in an easier way of simply shifting the existing temperature range of different phase structures (PPT temperatures).[6,13,22] The latter way seems to fit to the case of previously reported Ca and Zr (Sn) doped BT systems and Li, Ta, and Sb doped NKN systems in which no real MPB in the sense of crystallography has been so far formed because of an obvious dielectric anomaly corresponding to the transition between coexisting ferroelectric phases below T_c can be detected in permittivity versus temperature curves.[5,6,12,23,24]

Here, we reported a lead-free piezoelectric compound of (0.9-x)$NaNbO_3$-0.1$BaTiO_3$-x$CaZrO_3$ ((0.9-x)NN-0.1BT-xCZ), which shows desirable piezoelectric and electromechanical properties, particularly with an excellent temperature insensitivity in a relatively wide temperature range. This achievement was fundamentally ascribed to the finding of a composition-axis vertical MPB, as evidenced by a few religious structural analyses by means of the Rietveld refinements, synchrotron x-ray diffraction, and transmission electron microscopy together with the measurement of temperature dependent electrical properties.

The (0.9-x)NN-0.1BT-xCZ ceramics were prepared by a solid-state reaction method. The powders were mixed thoroughly in ethanol using zirconia balls for 12 h. The powder mixture was ball-milled again for 24 h after calcination at 1000 °C for 5 h, and then pressed into disk samples with a diameter of 10 mm under 100 MPa using polyvinyl alcohol as a binder. The disk samples were well sintered at 1250–1300 °C

[a]Author to whom correspondence should be addressed. Electronic addresses: piezolab@hfut.edu.cn and rzzuo@hotmail.com. Tel.: 86-551-62905285. FAX: 0086-551-62905285.

for 2 h in air after burning out the binder at 550 °C for 4 h (>96% theoretical densities). The samples were poled under a dc field of 4 kV mm^{-1} for 30 min at room temperature in a silicone oil bath.

The room-temperature phase structure was analyzed by a powder x-ray diffractometer (XRD, D/MAX-RB, Rigaku, Tokyo, Japan) using a Cu Kα radiation ($\lambda = 1.5406$ Å). Rietveld refinements were performed by using the program GSAS. Moreover, *in-situ* x-ray measurements of powder samples were taken at beam line 14B1 ($\lambda = 1.2378$ Å) at Shanghai Synchrotron Radiation Facility (SSRF). Measurements were performed at different temperatures by high-resolution θ–2θ step-scans using a Huber 5021 six-circle diffractometer with a NaI scintillation detector. The peak shape and the background were fitted by a pseudo Voigt function and a polynomial function, respectively.

Dielectric properties as a function of temperature and frequency were measured by an LCR meter (Agilent E4980A, Santa Clara, CA). The quasi-static piezoelectric constant d_{33} was measured by a Berlincourt-meter (YE2730A, Sinocera, Yangzhou, China) and the planar electromechanical coupling factor k_p was determined by a resonance-antiresonance method with an impedance analyzer (PV70A, Beijing Band ERA Co., Ltd. China). The polarization versus electric field (P–E) loops and bipolar/unipolar strain versus electric field (S–E) curves were measured at 1 Hz by using a ferroelectric measuring system (Precision multiferroelectric, Radiant Technologies Inc., Albuquerque, NM) connected with an accessory laser interferometer vibrometer (AE SP-S 120 E, SIOS Meβtechnik, GmbH, Ilmenau, Germany). Temperature-dependent k_p, P–S, and S–E curves were measured on a high-temperature probing stage (HFS600E-PB2, Linkam Scientific Instruments, Tadworth, UK). The domain morphology observation and selected area electron diffraction (SAED) were performed on a field-emission transmission electron microscope (FE-TEM, JEM-2100F, JEOL, Japan) operating at 200 kV.

A single perovskite-structured solid solution can be seen for all (0.9-x)NN-0.1BT-xCZ ceramics (see Figure S1).[25] An obvious (200) splitting indicated a typical T phase structure, which was found to become weak gradually with increasing x, and then to merge into a single one as x is beyond 0.03. A Rietveld refinement on full profiles of XRD patterns was performed to identify the crystal symmetry of each phase, as shown in Fig. 1(a) for a few selected samples. The refined structural parameters and various agreement factors were also listed (see Table S1).[25] The $x = 0$ sample was identified to be a single T phase with a space group of P4 mm, which was maintained up to $x = 0.02$. In the composition range of $0.02 \le x \le 0.03$, complex diffraction patterns could not be appropriately indexed with an either R or T symmetry. Instead, the refinement best fits to a combination of P4 mm and R3c space groups with an $R_p = 7.52\%$ for the $x = 0.025$ composition. As $x > 0.03$, a single phase could be well indexed once again according to an R cell with an R3c symmetry, which exhibits a doubled unit-cell structure probably owing to the oxygen octahedral antiphase tilting along the [111] pseudo-cubic (PC) axis (labeled as $a^-a^-a^-$ tilt). It is usually believed that oxygen octahedral tilting in perovskites is likely to occur as the tolerance factor t is below 0.985, as observed in BNT and PZT compositions[26,27] (see Figure S2).[25] With further increasing x larger than 0.035, a PC phase with a space group of $Pm\bar{3}m$ can be identified. It is evident that

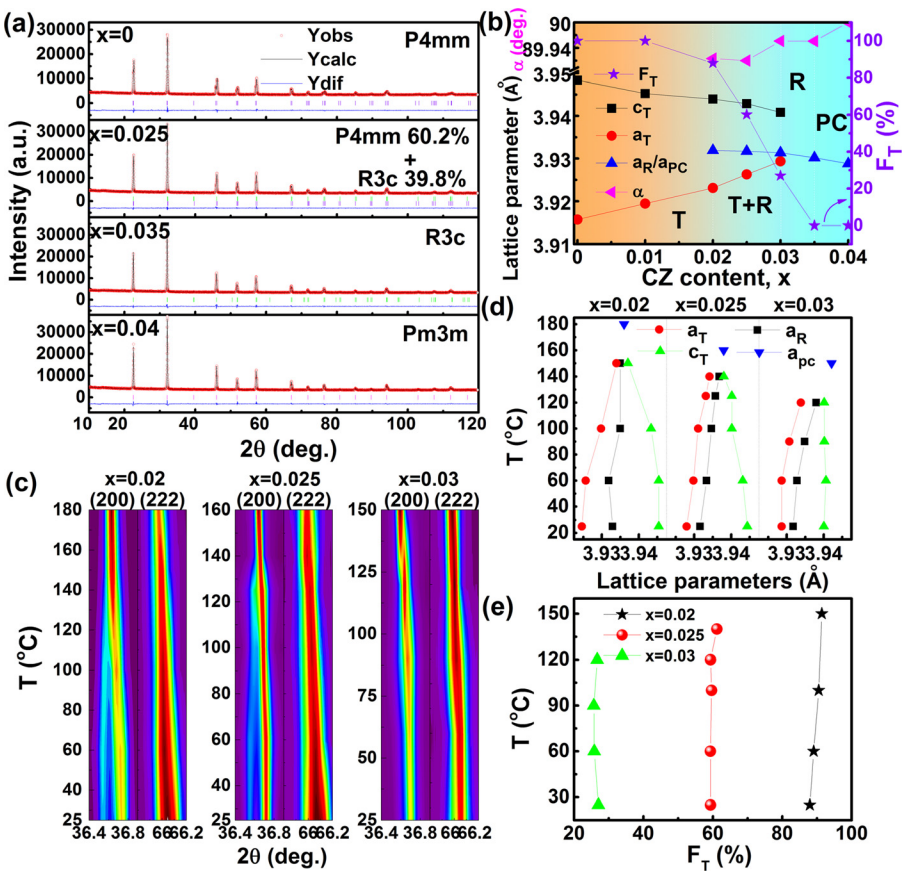

FIG. 1. Composition and temperature dependent phase structures of (0.9-x)NN-0.1BT-xCZ ceramics: (a) the Rietveld analysis results of XRD patterns for a few compositions as indicated, (b) the lattice parameters and the fraction of T phase (F_T) as a function of x, (c) the evolution of both (200) and (222) reflections with increasing temperature for three selected compositions, (d) lattice parameters of three typical compositions with temperature, and (e) the F_T values of three typical compositions with temperature.

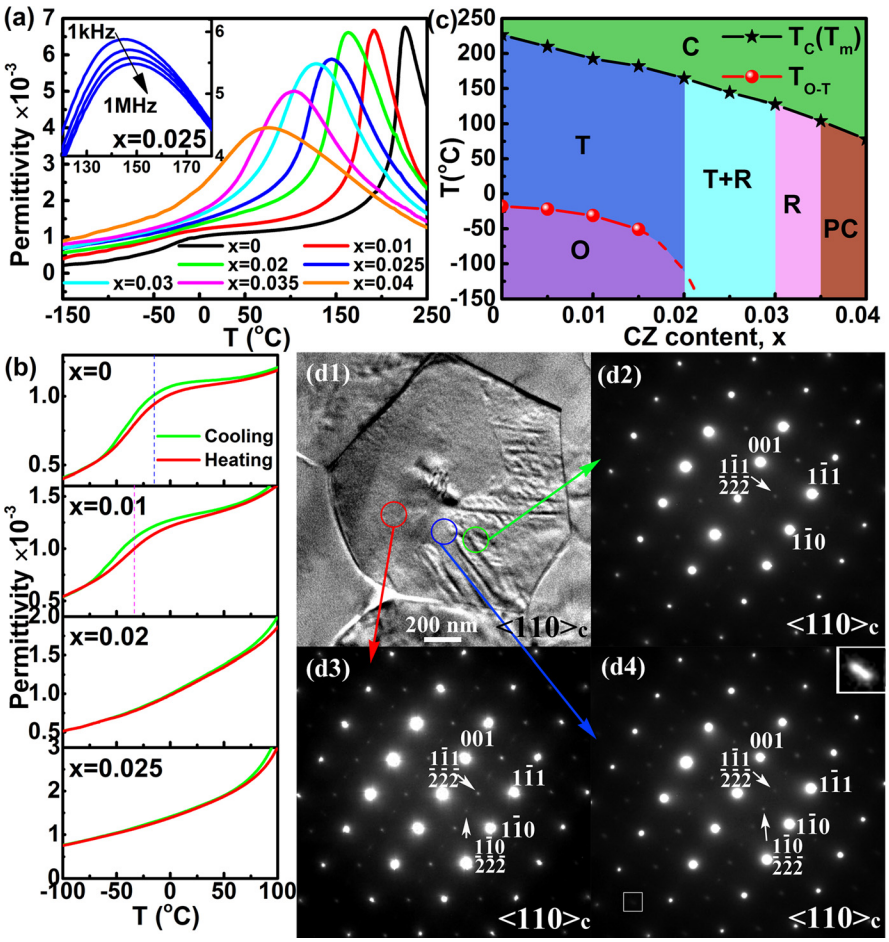

FIG. 2. Composition and temperature phase diagram of (0.9-x)NN-0.1BT-xCZ ceramics: (a) dielectric permittivity at 1 kHz of different compositions in the temperature range from −150 °C to 250 °C; the inset shows the frequency-dependent permittivity around the dielectric maxima for the x = 0.025 composition, (b) permittivity versus temperature curves at 1 kHz recorded during heating and cooling, (c) composition-temperature phase diagram of (0.9-x)NN-0.1BT-xCZ ceramics in which different phase zones were indicated, and ((d-1)–(d-4)) domain morphology and structural analysis of the x = 0.025 composition: (d-1) bright-field TEM image and (d-2)–(d-4) the corresponding SAED patterns along ⟨110⟩c measured in the neighboring areas as circled within one grain; the inset on upper-right corner in d-4 shows the enlarged diffraction spots as marked by a white square on the lower-left corner for clearly showing the spot splitting (elongation).

the addition of CZ induced an obvious phase transformation from a pure T phase, coexistence of R and T, then a pure R phase, and finally to a pure PC phase. Through the Rietveld refinement, the lattice parameters and the fraction of the T phase (F_T) of all derived phases within the studied composition range are shown in Fig. 1(b). The phase coexistence of R and T was found to exist in a narrow composition range of x = 0.02−0.03. The decreased tetragonality of T phases was accompanied by a reduced F_T value, which would be consistent with the variation of the T_c value.

The thermal stability of the phase structure for compositions in the proximity of R and T phase coexistence zone was investigated by means of synchrotron XRD measurements on two typical Bragg reflections, as shown in Fig. 1(c). These diffraction lines measured during increasing temperatures above the corresponding T_c values were analyzed by peak profile fitting (see Figure S3).[25] The initial R and T phase coexistence for x = 0.02, 0.025, and 0.03 samples was found to remain up to the proximity of their respective T_c values, above which all three samples became a single PC phase, as more clearly seen in Fig. 1(d). Although the tetragonality of T phases decreased with increasing temperature, yet their F_T values kept almost constant before their Curie points (Fig. 1(e)), strongly suggesting that the R and T phase boundary in the present study should be almost vertical to the composition axis. This extremely differs from those observed in previously reported NKN-based lead-free piezoelectric ceramics where the phase fraction of R, O, or T phases is seriously temperature sensitive.[12–14]

Fig. 2(a) shows the dielectric permittivity versus temperature (ε-T) curves of all the studied compositions. Their tan δ values can be seen in Figure S4. Most of the compositions exhibited an additional dielectric anomaly in additional to an obvious ferroelectric-paraelectric phase transition near T_c. Evidently, T_c decreased monotonously with increasing x. The dielectric anomaly hump at lower temperatures was clearly observed, particularly for compositions with x<0.02. This anomaly peak was believed to be a result of the O-T PPT. The x = 0 sample was reported to have a PPT from O to T at ∼−15 °C owing to the effect of BT addition on PPT temperatures of NN.[28] Considering this kind of PPT should belong to the first-order phase transition and exhibit an obvious thermal hysteresis effect, the ε-T curves were thus measured in the proximity of the low-temperature phase transition during both heating and cooling, as shown in Fig. 2(b). The PPT temperature, which can be estimated by using the intersection point of two tangent lines of 1/ε versus T curves (see Figure S5),[25] was found to be slightly shifted to lower temperatures, instead of high-temperature zones. Therefore, O phases can not appear at higher temperatures in the current system. This indicates that the addition of CZ thermodynamically played a role in stabilizing the T phases within a certain composition range although the tetragonality of T phases was reduced. However, the O-T PPT was not observed any more within the measuring temperature range, but a flat ε-T curve was seen for x ≥ 0.02 compositions below their T_c values. That is to say, below T_c there is not any thermal induced phase transition between R, T, or O not only for single-phase compositions (x > 0.03) but

also for R and T phase coexisted compositions ($0.02 \leq x \leq 0.03$). In other words, R and T phases coexisting in these compositions cannot be thermally transformed into each other. This is essentially different from those observed in BT-based or NKN-based lead-free ceramics where R-T, O-T, or R-O PPB was formed by simply shifting the PPT temperatures through chemical modifications.[11,12] Thereby, the R and T phase coexistence in the current study is morphotropic in nature, and only compositionally induced, as usually observed in conventional PZT ceramics. According to the aforementioned analyses, a temperature-composition phase diagram of (0.9-x)NN-0.1BT-xCZ ceramics was proposed, as shown in Fig. 2(c). The phase diagram is characterized by a vertical MPB zone separating ferroelectric T and R phases.

The bright-field domain morphology of the $x = 0.025$ sample with an R and T phase coexistence is shown in Fig. 2(d-1). Two kinds of domain configurations, such as tweed-like domains and polar nanodomains, can be observed. The refined domain morphology can well explain the formation of a weak dielectric relaxation behavior in the (0.9-x)NN-0.1BT-xCZ system with increasing x, as observed in the inset of Fig. 2(a). The tweed-like domains and polar nanodomains should originate from T phases and R phases, respectively, as can be confirmed by SAED patterns (Figs. 2(d-2)–(d-4)) along the ⟨110⟩c zone axis within a single grain (Fig. 2(d-1)). All of them exhibit obvious superstructure reflections, such as 1/2{ooo} and/or 1/2{ooe}, where o and e denote the odd and even Miller indices. In Fig. 2(d-2) observed from the marked region of Fig. 2(d-1), the 1/2{ooo} typed superstructure reflections were observed, which should correspond to the occurrence of an R3c symmetry with an antiphase octahedral tilting.[29,30] Fig. 2(d-3) shows the SAED pattern from the region (tweed-like domain zone) as indicated in Fig. 2(d-1). Two kinds of weak superstructure reflections such as 1/2{ooo} and 1/2{ooe} were detected probably because of the locally antiferrodistortive structure[31] in the NN-BT binary system, although none of any superstructure reflections can be generally seen in a T phase with a space group of P4 mm. NN is known to be a typical antiferroelectric at room temperature, exhibiting an obvious 1/4{ooe} superstructure reflection.[32,33] The addition of 10 mol. % BT with a strong ferroelectricity would destroy the antiferroelectric ordering state of NN into a ferroelectric ordering state with T symmetry.[28] However, an antiferrodistortive structure still exists at a microscopic scale and consists of tilting of the oxygen octahedra surrounding the B cation with a coherence length of the scale of the doubled unit cell,[34] in which the 1/2{ooe} reflections may originate from the doubled unit cells with antiparallel B-site cation displacement, and the 1/2{ooo} reflections are related to locally ordered oxygen octahedral tilting. This kind of microscopically antiferrodistortive structure may still exist at even higher temperatures although its coherence length will be accordingly reduced.[35] By comparison, the diffraction pattern of Fig. 2(d-4) from the crossover of the tweed domains (T phase) and polar nanodomains (R phase) can be found to exhibit an elongation (or splitting) of 1/2{ooo} diffraction spots, which is more pronounced for high Miller indices as shown in the inset of Fig. 2(d-4). The splitting of diffraction spots confirms that the 1/2{ooo} reflections in the R phase (Fig. 2(d-2)) have a different origin from that in the T phase (Fig. 2(d-3)), further indicating the coexistence of R and T phases in the $x = 0.025$ sample.

Room-temperature P-E loops and bipolar and unipolar S-E curves of (0.9-x)NN-0.1BT-xCZ ceramics are plotted in Figs. 3(a)–3(c). Well-saturated P-E loops and butterfly-shaped S-E curves indicated a typical ferroelectric nature at room temperature. Both coercive field E_c and remanent polarization P_r were found to decline with the substitution of CZ, because of both the reduction of tetragonality and the decrease of the T phase fraction in comparison to the R phase. As shown in Fig. 3(d), piezoelectric and electromechanical properties reached their maximum values of high-field piezoelectric coefficient d_{33}^* (S_{max}/E_{max}) ~240 pm V^{-1}, quasi-static d_{33} ~231 pC N^{-1}, and k_p ~35% in the composition of $x = 0.025$, which was located within the MPB of this system. This is because the R-T phase coexistence would cause the instability of the polarization state, such that the polarization vectors can be more easily rotated by external electric fields. Furthermore, the existence of nanodomains in the MPB composition would also favor high piezoelectric activities as a result of the reduced domain wall energy. With further increasing x, piezoelectric properties obviously decreased owing to the weakening of ferroelectricity caused by the formation of the R ($x = 0.035$) and PC relaxor phases ($x > 0.035$).

The thermal stability of ferroelectric and piezoelectric properties was evaluated by measuring temperature-dependent P (S) values of the $x = 0.025$ sample and d_{33} (k_p) values of different compositions. As shown in Fig. 4(a), the saturated P-E loop as well as butterfly-shaped S-E curve for the $x = 0.025$ sample could be maintained till 140 °C (very close to its T_c), which is different from some BNT based lead-free relaxor ferroelectrics in which below T_c (or T_m, the temperature at the dielectric maxima), there is a ferroelectric to relaxor phase transition temperature (T_{fr}) or a nonergodic to ergodic phase transition temperature (T_f) corresponding to a depolarization process at a relatively low temperature. The

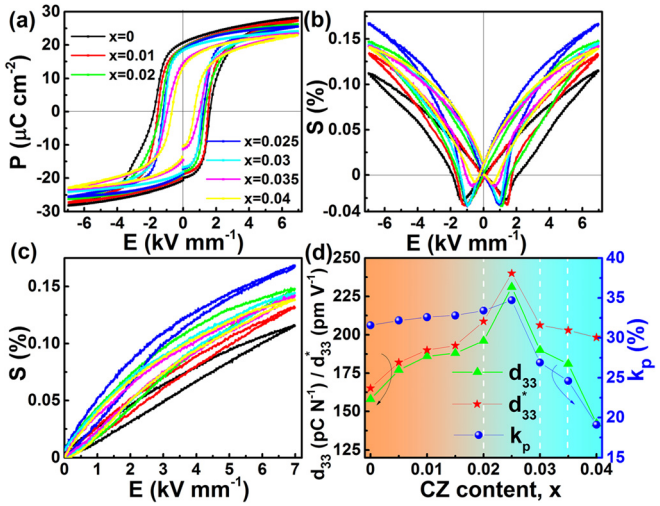

FIG. 3. Composition dependent ferroelectric and piezoelectric properties at room temperature: (a) P–E loops at 1 Hz, (b) bipolar S-E loops at 1 Hz, and (c) unipolar S-E curves at 1 Hz. Note that all P-E and S-E loops were measured from the non-first cycle of the measurement, and (d) high-field piezoelectric coefficient d_{33}^*, quasi-static d_{33}, and coupling factor k_p of (0.9-x)NN-0.1BT-xCZ ceramics.

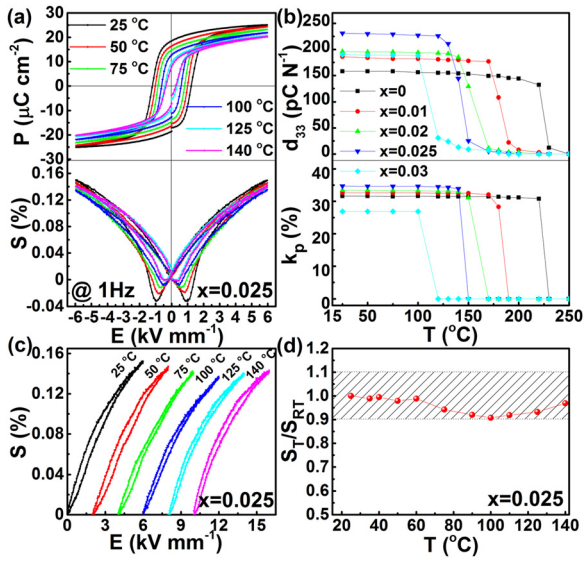

FIG. 4. Temperature dependent ferroelectric and piezoelectric properties of (0.9-x)NN-0.1BT-xCZ ceramics: (a) the P-E and bipolar S-E loops for the $x = 0.025$ composition at various temperatures, (b) thermal stability of d_{33} and k_p values; note that the d_{33} values were measured at room temperature after annealing at different temperatures for 20 min. Samples are open circuited during annealing but short circuited before d_{33} is re-measured. The disk sample dimensions are ~8.4 mm × ~0.5 mm and ~8.4 mm × ~3 mm for the k_p and d_{33} measurement, respectively; (c) unipolar S-E curves of the $x = 0.025$ sample at different temperatures, and (d) relative variation of the strain with respect to its room-temperature value S_{RT} of the $x = 0.025$ ceramic.

decrease in E_c, P_r, and negative strain S_{neg} with increasing temperature can be easily explained by the decrease in the ferroelectricity as T_c is approached. Fig. 4(b) shows the temperature dependence of piezoelectric and electromechanical properties of a few selected compositions. All selected compositions within the studied composition range displayed a good thermal stability of both d_{33} and k_p values up to their respective T_c. The temperature-insensitive piezoelectric properties can be basically attributed to the temperature-stable phase structure (Figs. 1(d) and 1(e)). Particularly, excellent piezoelectric properties of $d_{33} = 231$ pC N^{-1} and $k_p = 35\%$ can be kept stable till 140 °C during annealing for the composition of $x = 0.025$, further illustrating a temperature-insensitive R-T MPB. In addition, a thermal-insensitive large electrostrain of ~0.15% at 6 kV/mm with a rather small strain hysteresis (less than 15%) can be also obtained in the $x = 0.025$ composition in the temperature range of 25 °C ~140 °C, as shown in Fig. 4(c). The variation of the strain value in the studied temperature range is within ±10% of its room-temperature value, as indicated in Fig. 4(d), which is much better than most of BNT-, BT- or NKN-based lead-free piezoelectric systems and comparable to the classical PZT-based ceramics. The combination of good electromechanical properties with their desirable thermal stability in a wide temperature range would make (0.9-x)NN-0.1BT-xCZ ceramics a very promising material for piezoelectric device applications.

In summary, we reported a morphotropic NN-BT-CZ ternary lead-free piezoelectric ceramic, analogous to traditional PZT materials but obviously different from BT-based or NKN-based lead-free systems. The essence of the composition-axis vertical phase boundary between P4 mm and R3c was clearly identified to be morphotropic, providing a solid structural base for good piezoelectric and electromechanical properties and especially their excellent thermal stability in a wide temperature range. The current study might open a good opportunity for speeding up further development and industrial applications of environmentally friendly piezoelectric materials.

This work was supported by the National Natural Science Foundation of China (Grants Nos. 51472069, U1432113, 51402079, 51332002) and the Anhui Provincial Natural Science Foundation (1508085JGD04).

[1]M. Ahart, M. Somayazulu, R. E. Cohen, P. Ganesh, P. Dera, H. K. Mao, R. J. Hemley, Y. Ren, P. Liermann, and Z. Wu, Nature **451**, 545 (2008).
[2]H. Fu and R. E. Cohen, Nature **403**, 281 (2000).
[3]W. Cao and L. E. Cross, Phys. Rev. B **47**, 4825 (1993).
[4]W. F. Zhou, P. Chen, and Q. Pan, Adv. Mater. **27**, 6349 (2015).
[5]W. F. Liu and X. B. Ren, Phys. Rev. Lett. **103**, 257602 (2009).
[6]Y. Saito, H. Takao, T. Tani, T. Nonoyama, K. Takatori, T. Homma, T. Nagaya, and M. Nakamura, Nature **432**, 84 (2004).
[7]J. G. Wu, D. Q. Xiao, and J. G. Zhu, Chem. Rev. **115**, 2559 (2015).
[8]D. Schütz, M. Deluca, W. Krauss, A. Feteira, T. Jackson, and K. Reichmann, Adv. Funct. Mater. **22**, 2285 (2012).
[9]G. Singh, V. S. Tiwari, and P. K. Gupta, Appl. Phys. Lett. **102**, 162905 (2013).
[10]M. Acosta, N. Khakpash, T. Someya, N. Novak, W. Jo, H. Nagata, G. A. Rossetti, Jr., and J. Rödel, Phys. Rev. B **91**, 104108 (2015).
[11]D. S. Keeble, F. Benabdallah, P. A. Thomas, M. Maglione, and J. Kreisel, Appl. Phys. Lett. **102**, 092903 (2013).
[12]R. Z. Zuo and J. Fu, J. Am. Ceram. Soc. **94**, 1467 (2011).
[13]J. Fu, R. Z. Zuo, and X. Y. Gao, Appl. Phys. Lett. **103**, 182907 (2013).
[14]E. K. Akdoğan, K. Kerman, M. Abazari, and A. Safari, Appl. Phys. Lett. **92**, 112908 (2008).
[15]S. J. Zhang, R. Xia, H. Hao, H. Liu, and X. T. R. Shrout, Appl. Phys. Lett. **92**, 152904 (2008).
[16]T. A. Skidmore, T. P. Comyn, and S. J. Milne, Appl. Phys. Lett. **94**, 222902 (2009).
[17]T. Karaki, T. Katayama, K. Yoshida, S. Maruyama, and M. Adachi, Jpn. J. Appl. Phys., Part 1 **52**, 09KD11 (2013).
[18]R. Baba, T. Karaki, and T. Fujii, J. Adv. Dielectr. **6**, 1650008 (2016).
[19]Y. M. Jin, Y. U. Wang, A. G. Khachaturyan, J. F., Li, and D. Viehland, Phys. Rev. Lett. **91**, 197601 (2003).
[20]K. A. Schönau, L. A. Schmitt, M. Knapp, H. Fuess, R. A. Eichel, H. Kungl, and M. J. Hoffmann, Phys. Rev. B **75**, 184117 (2007).
[21]T. Asada and Y. Koyama, Phys. Rev. B **75**, 214111 (2007).
[22]R. P. Wang, H. Bando, and M. Itoh, Appl. Phys. Lett. **95**, 092905 (2009).
[23]X. P. Wang, J. G. Wu, D. Q. Xiao, J. G. Zhu, X. J. Cheng, T. Zheng, B. Y. Zhang, X. J. Lou, and X. J. Wang, J. Am. Chem. Soc. **136**, 2905 (2014).
[24]E. Hollenstein, M. Davis, D. Damjanovic, and N. Setter, Appl. Phys. Lett. **87**, 182905 (2005).
[25]See supplementary material at http://dx.doi.org/10.1063/1.4958937 for the composition and temperature dependent crystal structure, tolerance factor t as a function of composition, and inverse dielectric permittivity and the loss tangent of the samples as a function of temperature.
[26]T. Rojac, S. Drnovsek, A. Bencan, B. Malic, and D. Damjanovic, Phys. Rev. B **93**, 014102 (2016).
[27]W. C. Lee, C. Y. Huang, L. K. Tsao, and Y. C. Wu, J. Eur. Ceram. Soc. **29**, 1443 (2009).
[28]J. T. Zeng, K. W. Kwok, and H. L. W. Chan, J. Am. Ceram. Soc. **89**, 2828 (2006).
[29]C. Ma, H. Z. Guo, S. P. Beckman, and X. L. Tan, Phys. Rev. Lett. **109**, 107602 (2012).
[30]H. T. Huang, L. M. Zhou, J. Guo, H. H. Hng, J. T. Oh, and P. Hing, Appl. Phys. Lett. **83**, 3692 (2003).
[31]X. H. Dai, Z. K. Xu, and D. Viehland, J. Am. Ceram. Soc. **78**, 2815 (1995).
[32]Y. Cai, F. Phillipp, A. Zimmermann, L. Zhou, F. Aldinger, and M. Rühle, Acta Mater. **51**, 6429 (2003).
[33]J. Chen and D. Feng, Phys. Status Solidi A **109**, 171 (1988).
[34]P. Aguado-Puente, P. García-Fernández, and J. Junquera, Phys. Rev. Lett. **107**, 217601 (2011).
[35]B. Rechav, Y. Yacoby, E. A. Stern, J. J. Rehr, and M. Newville, Phys. Rev. Lett. **72**, 1352 (1994).